SIAM J. APPL. MATH.
Vol. 81, No. 1, pp. 129–152

MODELING THE EFFECT OF SURFACTANT ON DROPLET BREAKUP IN A TURBULENT FLOW*

RACHEL M. PHILIP†, IAN J. HEWITT†, AND PETER D. HOWELL†

Abstract. In many industrial applications oil drops suspended in water are broken down by turbulent fluid motion, assisted by the addition of surfactants. In this paper, we develop a model for the interaction between droplet breakup and surfactant behavior in a homogeneous turbulent flow. We derive equations for the evolution of droplet size distribution, surfactant concentration, and surface tension. Our resulting model is analyzed using both asymptotic and numerical methods. We find that the large-time behavior is highly dependent on the history of the drop-surfactant interaction, and we identify distinct phases in the breakup dynamics. The model is then used to investigate how increasing the concentration of surfactant promotes enhanced droplet breakup and thus increases the proportion of smaller droplets. We also explore varying the method of surfactant addition and find that there may be advantages to adding the surfactant gradually rather than all at once. These results can be used to optimize surfactant application in industrial processes.

Key words. droplet breakup, surfactants, asymptotic analysis

AMS subject classifications. 35R09, 35C20, 76T99

DOI. 10.1137/20M1321851

1. Introduction.

In an oceanic oil spill, oil drops suspended in water are broken down by turbulent fluid motion. To accelerate the production of smaller droplets, which are more easily dispersed and consumed by microorganisms [2, 13], surfactants are added to reduce the oil-water surface tension and facilitate droplet breakup [22]. A similar process occurs in various other industrial applications, for example, oil-in-water emulsions, which are formed and stabilized by intensive stirring and adding surfactants [10]. Therefore, it is important to understand the interaction between surfactants and turbulent droplet breakup.

The breakup of drops in a turbulent flow, without the presence of surfactants, has been studied extensively, both experimentally and theoretically. Scaling laws, supported by empirical data, have been used to predict the mean drop size as well as the droplet size distribution [5, 12, 13, 14]. Another common approach is to use population balance models to track the evolution of the droplet size distribution over time [7, 16, 17, 23, 26]. In these population type models, the effect of a surfactant on the drop size distribution has been addressed by reducing the surface tension to a small constant value [24, 25]. However, this approach neglects the mechanism by which surfactant addition changes the surface tension and how this is influenced by the evolution of the drop size distribution.

Surfactant molecules possess a hydrophilic (water-attracting) head and hydrophobic (water-repelling) tail. Rather than remaining dissolved in a bulk water phase, it is more energetically favorable for a surfactant monomer to adsorb to an oil-water interface, with the hydrophobic tail expelled from the water. This action reduces the local oil-water surface tension. If the bulk surfactant concentration is large, the

*Received by the editors March 9, 2020; accepted for publication (in revised form) October 22, 2020; published electronically January 21, 2021.
https://doi.org/10.1137/20M1321851
Funding: This publication is based on work supported by the EPSRC Centre For Doctoral Training in Industrially Focused Mathematical Modelling (EP/L015803/1) in collaboration with BP.
†OCIAM, Mathematical Institute, Andrew Wiles Building, Oxford, OX2 6GG, UK (philip@maths.ox.ac.uk, hewitt@maths.ox.ac.uk, howell@maths.ox.ac.uk).

monomers also form aggregates in the bulk called micelles. A micelle consists of anywhere between 15 and 100 monomers [1, 18] grouped together so that the hydrophilic heads are in contact with the surrounding water while the hydrophobic tails are in the interior. The bulk surfactant concentration above which these micelles form is called the critical micelle concentration. Simple mathematical models for the concentration of surfactant monomers and micelles in the bulk, and their effect on the concentration of surfactant adsorbed at a single interface, may be found, for example, in [3, 4, 6].

In this paper we combine and extend these approaches to understand the effect of surfactant on the turbulent breakup of oil droplets. For simplicity, we assume spatial homogeneity; extensions to describe droplet breakup in a spatially varying turbulent jet can be found in [20]. We also neglect the detailed structure of the underlying turbulent flow and assume that the relevant hydrodynamic quantity that affects breakup is the turbulent energy dissipation rate [8, 12, 20]. We use a droplet population model to track changes in the drop size distribution with time. The breakup rate in this model depends on both the energy of the turbulent flow and the surface concentration of the surfactant, which controls the oil-water surface tension. The model also incorporates the interaction of this surface concentration with the bulk surfactant concentrations of monomers and micelles, which are all coupled to the drop-size dynamics.

In section 2, we derive the coupled model for droplet breakup and drop-surfactant interaction. The constitutive laws used to model the breakup rates are described in section 3. In section 4, we solve the model, assuming a simplified breakup rate, which is independent of droplet size, and we explore the behavior of the solutions with the help of an asymptotic analysis. In section 5, we extend the results to a more general breakup rate. In section 6, we use the model to examine the effect of varying the concentration of surfactant added and the method of surfactant addition. We discuss the implications of our results in section 7.

2. Mathematical modeling.

2.1. Droplet breakup. We consider a spatially homogeneous volume of water with a low oil fraction. The oil and water have similar densities and viscosities and are well-mixed. We suppose that the fluid is subject to homogeneous turbulent motion, which is characterized by the constant turbulent energy dissipation rate ϵ.

The distribution of oil droplets with volume v at time t is denoted by $\phi(v,t)$. Specifically, we define ϕ as the distribution of volume fraction, so the total volume fraction of oil is given by

$$\Phi(t) = \int_0^\infty \phi(v,t)\,\mathrm{d}v. \tag{2.1}$$

For later reference we also note that, assuming approximately spherical droplets, the droplet surface area per unit volume is given by

$$S(t) = (6\sqrt{\pi})^{2/3} \int_0^\infty \frac{\phi}{v^{1/3}}\,\mathrm{d}v. \tag{2.2}$$

We let $\gamma(\tilde{v},\epsilon,\sigma)$ denote the rate at which drops of volume $\tilde{v}$ break up, assumed to be a function of drop size, turbulent energy dissipation ϵ, and surface tension σ. For notational brevity, the dependence of γ on ϵ will henceforth be suppressed. We let $\chi(v,\tilde{v})$ be the daughter size distribution, representing the expected proportion of the volume of a $\tilde{v}$-sized drop that becomes v-sized droplets upon breakup. A drop of

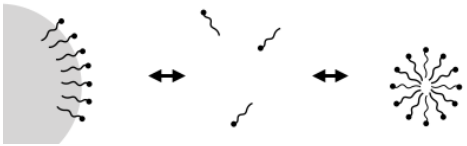

FIG. 1. *Schematic of interactions between the three populations of surfactant: adsorbed surfactant on the surface of the oil droplets (surface concentration* Γ*), free surfactant monomers in the bulk (concentration* c*), and micelles (concentration* c_m*).*

volume $\tilde{v}$ can only break up into drops with smaller volume, so that $\chi(v, \tilde{v}) \equiv 0$ for $v > \tilde{v}$, and conservation of oil implies the identity

$$\int_0^{\tilde{v}} \chi(v, \tilde{v})\, \mathrm{d}v \equiv 1. \tag{2.3}$$

Note that χ is assumed to depend only on droplet size, with all other effects captured by γ. Specific choices for the forms of γ and χ are discussed in section 3.

The droplet volume fraction, $\phi(v, t)$, is governed by the master equation

$$\frac{\partial \phi}{\partial t}(v, t) = -\gamma(v, \sigma)\phi(v, t) + \int_v^{\infty} \gamma(\tilde{v}, \sigma)\chi(v, \tilde{v})\phi(\tilde{v}, t)\, \mathrm{d}\tilde{v}. \tag{2.4}$$

The first term on the right-hand side of (2.4) corresponds to drops of volume v breaking up; the second represents the process by which larger drops break into those of volume v. Taking the integral of (2.4) over all drop sizes and using (2.3) shows that Φ is constant, confirming that the total volume fraction of oil in the system is conserved. The model (2.4) has been used in the literature in a similar form [16, 17, 23, 26].

2.2. Surfactant. To determine the surface tension, σ, we now consider drop-surfactant interactions (Figure 1). We measure the bulk concentration of surfactant monomers, c, and micelles, c_m, in units of moles per unit volume, while the surface concentration, Γ, is measured in moles of adsorbed surfactant per unit area. We make the simplifying assumption that the surface concentration, Γ, is independent of drop size, so the moles of adsorbed surfactant per unit volume is ΓS, where S is the surface area fraction defined in (2.2).

The surface tension depends on the surface concentration, and we model this dependence using the Frumkin equation [6],

$$\sigma = \sigma_0 + RT\Gamma_m \log\left(1 - \frac{\Gamma}{\Gamma_m}\right), \tag{2.5}$$

where R is the gas constant, T is the (assumed constant) temperature, and Γ_m is the theoretical maximum surface concentration. Equation (2.5) describes how, as the surface concentration increases, the surface tension decreases from its undisturbed value σ_0.

It remains to determine Γ by considering interactions between micelles, surfactant monomers, and adsorbed surfactant. Monomers can aggregate to form micelles, and the micelles can break up into monomers. These processes are modeled using the law of mass action,

$$\frac{dc_m}{dt} = k_0^+ c^{N_m} - k_0^- c_m, \tag{2.6}$$

where k_0^+ and k_0^- are the rates at which micelles form and break up, respectively. We suppose that all micelles consist of the same number N_m of monomers, which is typically large.

The exchange between bulk and adsorbed surfactant is modeled by the Langmuir–Hinshelwood equation [6] as

$$\frac{d(\Gamma S)}{dt} = k_a c \left(1 - \frac{\Gamma}{\Gamma_m}\right) S - k_d \Gamma S, \tag{2.7}$$

where k_a and k_d are parameters relating to the rates of adsorption and desorption, respectively. The presence of S inside the derivative on the left-hand side of (2.7) captures the depletion or accumulation of adsorbed surfactant due to changes in the available surface area.

Free monomers in the bulk are produced both when surfactant desorbs from the surface and when micelles break up, at a rate given by

$$\frac{dc}{dt} = -N_m k_0^+ c^{N_m} + N_m k_0^- c_m - k_a c \left(1 - \frac{\Gamma}{\Gamma_m}\right) S + k_d \Gamma S. \tag{2.8}$$

The total moles of surfactant per unit volume is given by

$$C = c + \Gamma S + N_m c_m. \tag{2.9}$$

Adding (2.6), (2.7), and (2.8) shows that C is conserved, and it is therefore taken to be a known constant C_0, which is set by the initial conditions. It is of particular interest to determine how drop breakup depends on the parameter C_0, i.e., on the total quantity of surfactant added to the system.

2.3. Nondimensionalization. We nondimensionalize using

(2.10a)

$$t = \tau t^*, \qquad \sigma = \sigma_0 \sigma^*, \qquad v = v_0 v^*, \qquad \phi = \frac{\Phi}{v_0}\,\phi^*, \qquad \gamma = \frac{1}{\tau}\,\gamma^*,$$

(2.10b)

$$\chi = \frac{1}{v_0}\,\chi^*, \quad c = c_{\mathrm{cmc}} c^*, \quad \Gamma = \Gamma_m \Gamma^*, \quad c_m = \frac{c_{\mathrm{cmc}}}{N_m}\,c_m^*, \quad S = \left(\frac{36\pi}{v_0}\right)^{1/3} \Phi S^*,$$

where τ is a characteristic breakup time-scale related to the underlying turbulent flow, σ_0 is the undisturbed surface tension, v_0 is a characteristic drop size, Φ is the total oil fraction, and c_{cmc} denotes the critical micelle concentration (CMC) introduced in section 1. As explained in [4], a suitable definition of the CMC may be obtained by considering the equilibrium of a monomer–micelle mixture in the absence of any free surfaces. From (2.6) and (2.9) in steady state with zero surface concentration, we obtain

$$\frac{C}{c_{\mathrm{cmc}}} = \frac{c}{c_{\mathrm{cmc}}} + \left(\frac{c}{c_{\mathrm{cmc}}}\right)^{N_m}, \tag{2.11}$$

where

$$c_{\mathrm{cmc}} = \left(\frac{k_0^-}{N_m k_0^+}\right)^{1/(N_m - 1)}. \tag{2.12}$$

Given that N_m is large, when $C < c_{\rm cmc}$ the final term in (2.11) (representing micelles) is negligibly small and $c \approx C$, while when $C > c_{\rm cmc}$ we have $c \approx c_{\rm cmc}$. Thus (2.11) is consistent with the identification of $c_{\rm cmc}$ as the CMC for the surfactant.

The resulting dimensionless equations, with asterisks dropped, are

$$\frac{\partial \phi}{\partial t}(v,t) = -\gamma(v,\sigma)\phi(v,t) + \int_v^\infty \gamma(\tilde{v},\sigma)\chi(v,\tilde{v})\phi(\tilde{v},t)\,\mathrm{d}\tilde{v}, \tag{2.13a}$$

$$S = \int_0^\infty \frac{\phi(v,t)}{v^{1/3}}\,\mathrm{d}v, \tag{2.13b}$$

$$\sigma = 1 + \theta \log(1-\Gamma), \tag{2.13c}$$

$$\frac{dc}{dt} = -\mathcal{K}_0\left[c^{N_m} - c_m\right] - \mathcal{K}_a\alpha\left[(1-\Gamma)cS - \eta\Gamma S\right], \tag{2.13d}$$

$$\frac{d(\Gamma S)}{dt} = \mathcal{K}_a\left[(1-\Gamma)cS - \eta\Gamma S\right], \tag{2.13e}$$

$$\frac{dc_m}{dt} = \mathcal{K}_0\left[c^{N_m} - c_m\right], \tag{2.13f}$$

$$\mathcal{C}_0 = c + \alpha\Gamma S + c_m \tag{2.13g}$$

with dimensionless parameters

$$\theta = \frac{RT\Gamma_m}{\sigma_0}, \qquad \mathcal{K}_0 = k_0^- \tau, \qquad \eta = \frac{k_d\Gamma_m}{k_a c_{\rm cmc}}, \tag{2.14a}$$

$$\alpha = \frac{(6\sqrt{\pi})^{2/3}\,\Phi\Gamma_m}{v_0^{1/3} c_{\rm cmc}}, \qquad \mathcal{K}_a = \frac{\tau k_a c_{\rm cmc}}{\Gamma_m}, \qquad \mathcal{C}_0 = \frac{C_0}{c_{\rm cmc}}. \tag{2.14b}$$

The algebraic relation (2.13g) may be used to eliminate one of the concentration variables, for example, c_m, and thus reduce (2.13d)–(2.13f) to a system of two differential equations for c and Γ, coupled to the drop size evolution equation (2.13a) by the surface area S.

2.4. Parameter values. The parameter θ measures the relative variation in surface tension due to changes in Γ, and its size depends primarily on the maximum surface concentration, a property of the particular surfactant [2, 6]. We assume that Γ does not exceed $1 - e^{-1/\theta}$, beyond which value (2.13b) would imply a negative surface tension. The rates at which monomers adsorb onto droplet surfaces, and at which micelles disassociate into monomers, are typically rapid compared to the breakup rate, so the two ratios $\mathcal{K}_0$ and $\mathcal{K}_a$ are expected to be large [6]. The parameter η represents the ratio of the rates of surfactant desorption and adsorption, which in most cases is relatively small [6, 9]. Finally, the ratio $\Gamma_m/c_{\rm cmc}$ measures the length-scale of the layer of surfactant monomers on the surface of the drops while $v_0^{1/3}$ represents a typical droplet diameter. Thus, α corresponds to how much surfactant is typically on the surface of the droplets compared to how much is in the bulk. The value of α is often quite small, indicating that the majority of the surfactant resides in the bulk, at least initially [6, 7, 9].

Estimated values of the dimensionless parameters for an example surfactant, dioctyl sulfosuccinate, are given in Table 1 [1, 2, 6, 9, 18, 19]. These parameters may vary significantly depending on the particular surfactant and application and thus throughout this paper illustrative values will be used.

TABLE 1
Typical values of dimensionless parameters for the example surfactant, dioctyl sulfosuccinate [1, 2, 6, 9, 18, 19].

Parameter	Value
N_m	$15 - 100$
θ	0.07-1.9
$\mathcal{K}_0$	25
η	0.0206
α	1.99×10^{-4}
$\mathcal{K}_a$	24

2.5. Initial conditions. Initially, we take the drop size to be log-normally distributed in v with mean at $v = 1$ in dimensionless variables, i.e.,

$$\phi(v,0) = \phi_0(v) = \frac{1}{v\sigma_v\sqrt{2\pi}} \exp\left(-\frac{\left(2\log v + \sigma_v^2\right)^2}{8\sigma_v^2}\right). \tag{2.15}$$

Here σ_v is the standard deviation of the associated normal distribution, related to the variance Δ of the initial size distribution by $\sigma_v^2 = \log(1+\Delta)$. In our simulations we take $\Delta = 0.1$.

For the majority of this paper we also assume that, at $t = 0$, all the surfactant is instantaneously added to the bulk; there is initially no adsorbed surfactant on the oil drops and the micelles and monomers in the injected surfactant are already in thermodynamic equilibrium with each other. Hence, the initial conditions are given by

$$c = c_0, \quad c_m = c_0^{N_m}, \quad \Gamma = 0 \quad \text{at } t = 0, \tag{2.16}$$

where $\mathcal{C}_0 = c_0 + c_0^{N_m}$.

3. Constitutive relations. To close the model (2.13a)–(2.13g), we must decide on the forms of the breakup rate, γ, and the daughter drop distribution, χ. Some progress can be made by dimensional analysis. Kolomogorov's local isotropic model of turbulence implies that turbulent energy fluctuations are a function of the energy dissipation rate ϵ and the wave-length of fluctuations [21]. We assume that droplet breakup is precipitated by turbulent fluctuations with wave-length comparable to the drop diameter $d = (6v/\pi)^{1/3}$ [12]. Then, by dimensional analysis, the corresponding pressure fluctuations are of order $\rho\epsilon^{2/3}d^{2/3}$, while the restoring capillary pressure is of order σ/d, where σ is the surface tension. The ratio of these two scalings yields the dimensionless Weber number

$$We = \rho\epsilon^{2/3}d^{5/3}\sigma^{-1} = \left(\frac{6}{\pi}\right)^{5/9} \rho\epsilon^{2/3}v^{5/9}\sigma^{-1}. \tag{3.1}$$

A rate constant that is independent of drop size is given by $\epsilon^{3/5}\rho^{2/5}\sigma^{-2/5}$. Therefore, a general dimensionally consistent form of the breakup rate is given by

$$\gamma = K_0\epsilon^{3/5}\rho^{2/5}\sigma^{-2/5}F(We), \tag{3.2}$$

where K_0 is a dimensionless constant and F is some function to be determined empirically. The simplest possibility is to take $F = 1$ in (3.2), and we shall explore the implications of this choice in section 4.

To suggest a more general form of the function F, we note that large droplets are not significantly affected by surface tension, implying that γ should be independent of σ at large v. However, the restoring force of surface tension makes drops increasingly difficult to break up with decreasing size, and some of the smallest droplets may be unable to break up at all. These properties are satisfied by setting

$$F(We) = We^{-2/5}\sqrt{1 - We_c/We}\,\mathcal{H}(1 - We_c/We), \tag{3.3}$$

as in [16, 17], where $\mathcal{H}$ is the Heaviside function and We_c is a critical Weber number, corresponding to a critical drop size v_c below which droplets do not break up.

We note that the posed form of the breakup rate (3.2) neglects the influence of viscosity μ in opposing droplet deformation and breakup, which is measured by the droplet capillary number $Ca = \mu\epsilon^{1/3}d^{1/3}/\sigma$ [5, 20]. Viscous effects may become relevant at very low values of the surface tension, e.g., when the surfactant concentration is significantly above the CMC, but for simplicity we do not include them here.

We nondimensionalize as in (2.10). Taking the time-scale τ as $\sigma_0^{2/5}\epsilon^{-3/5}\rho^{-2/5}/K_0$, the dimensionless version of (3.2) for $F = 1$ is simply

$$\gamma = \sigma^{-2/5}. \tag{3.4}$$

Alternatively, for the more complicated functional form (3.3), it is more natural to take $\tau = (6/\pi)^{2/9}v_0^{2/9}\epsilon^{-1/3}/K_0$, in which case the dimensionless breakup rate is

$$\gamma = v^{-2/9}\left(1 - b\sigma v^{-5/9}\right)^{1/2}\mathcal{H}\left(1 - b\sigma v^{-5/9}\right), \tag{3.5}$$

where

$$b = \frac{We_c\sigma_0(\pi/6)^{5/9}}{\rho\epsilon^{2/3}v_0^{5/9}} \tag{3.6}$$

is a rescaled version of the critical Weber number. In terms of this constant, the dimensionless critical droplet volume is $v_c = (b\sigma)^{9/5}$. Typical parameter values suggest $b = \mathcal{O}(10^{-3})$ [2, 7, 12, 16]; in our simulations we take $b = 0.5 \times 10^{-3}$.

The daughter drop distribution can be expressed as $\chi(v, \tilde{v}) = vN(v, \tilde{v})/\tilde{v}$, where $N(v, \tilde{v})$ is the expected number density of drops of volume v produced when a drop of volume $\tilde{v}$ breaks up. For simplicity, we take $N(v, \tilde{v})$ to be independent of v so the distribution of daughter drop sizes produced is uniform. Ensuring (2.3) is satisfied then determines

$$\chi(v, \tilde{v}) = \frac{2v}{\tilde{v}^2}. \tag{3.7}$$

Note that, although the number density of drops produced is uniform, the resulting volume distribution is a monotonically increasing function of daughter drop volume v.

4. Drop-size independent breakup rate.

4.1. Numerical solution. Here we present numerical solutions of the model (2.13), using the simplest constitutive relations (3.4) and (3.7) for the breakup rate and the daughter droplet size distribution.

In this case it is possible to resolve the drop-surfactant behavior without explicitly solving the integro-differential equation (2.13a) for ϕ. We multiply (2.13a) by v^n and

then integrate from $v = 0$ to $v = \infty$ to obtain

$$\frac{d}{dt}\left(\int_0^\infty v^n \phi \, \mathrm{d}v\right) = -\frac{n}{(n+2)\sigma^{2/5}} \int_0^\infty v^n \phi \, \mathrm{d}v. \tag{4.1}$$

Taking $n = 1$ and $n = -1/3$ yields equations for the mean drop size, $\overline{v} = \int_0^\infty v\phi \, \mathrm{d}v$, and droplet surface area, S, respectively. We obtain

$$\frac{d\overline{v}}{dt} = -\frac{\overline{v}}{3\sigma^{2/5}}, \qquad \frac{dS}{dt} = \frac{S}{5\sigma^{2/5}}, \tag{4.2}$$

which can be used along with (2.13b)–(2.13g) to solve for the surface tension, without explicitly solving for the drop size distribution. The surfactant problem thus reduces to the three coupled ODEs

$$\frac{d\overline{v}}{dt} = -\frac{\overline{v}}{3\sigma^{2/5}}, \tag{4.3a}$$

$$\frac{d\Gamma}{dt} = \mathcal{K}_a\left[(1-\Gamma)c - \eta\Gamma\right] - \frac{\Gamma}{5\sigma^{2/5}}, \tag{4.3b}$$

$$\frac{dc_m}{dt} = \mathcal{K}_0\left[c^{N_m} - c_m\right] \tag{4.3c}$$

with

$$\sigma = 1 + \theta \log(1-\Gamma), \tag{4.4a}$$

$$c = \mathcal{C}_0 - \alpha\Gamma S - c_m, \tag{4.4b}$$

$$S = S(0)\overline{v}^{-3/5}, \tag{4.4c}$$

where $S(0) = e^{2\sigma_v^2/9}$ is the initial value of S. The initial conditions are as outlined in subsection 2.5, i.e.,

$$\overline{v}(0) = 1, \qquad \Gamma(0) = 0, \qquad c_m(0) = c_0^{N_m}. \tag{4.5}$$

Once the surface tension has been determined using (4.3)–(4.4), the drop size distribution, given by (2.13a) subject to (2.15), may be calculated analytically in this simple case. In terms of a rescaled time variable τ given by

$$\tau = \int_0^t \sigma(\tilde{t})^{-2/5} \, \mathrm{d}\tilde{t}, \tag{4.6}$$

the master equation (2.13a) reduces to

$$\frac{\partial\phi}{\partial\tau}(v,\tau) + \phi(v,\tau) = 2v\int_v^\infty \frac{\phi(\tilde{v},\tau)}{\tilde{v}^2} \, \mathrm{d}\tilde{v}. \tag{4.7}$$

Taking a Laplace transform in τ, the solution of (4.7) may be found in the form

$$\phi(v,\tau) = e^{-\tau}\phi_0(v) + ve^{-\tau}\sqrt{2\tau}\int_v^\infty \frac{\phi_0(u)}{u^2} \frac{\mathrm{I}_1\left(2\sqrt{2\tau\log(u/v)}\right)}{\sqrt{\log(u/v)}} \, \mathrm{d}u, \tag{4.8}$$

where I_1 is the modified Bessel function of order one and $\phi_0(v) = \phi(v,0)$ is the initial droplet size distribution, which we take to be given by (2.15).

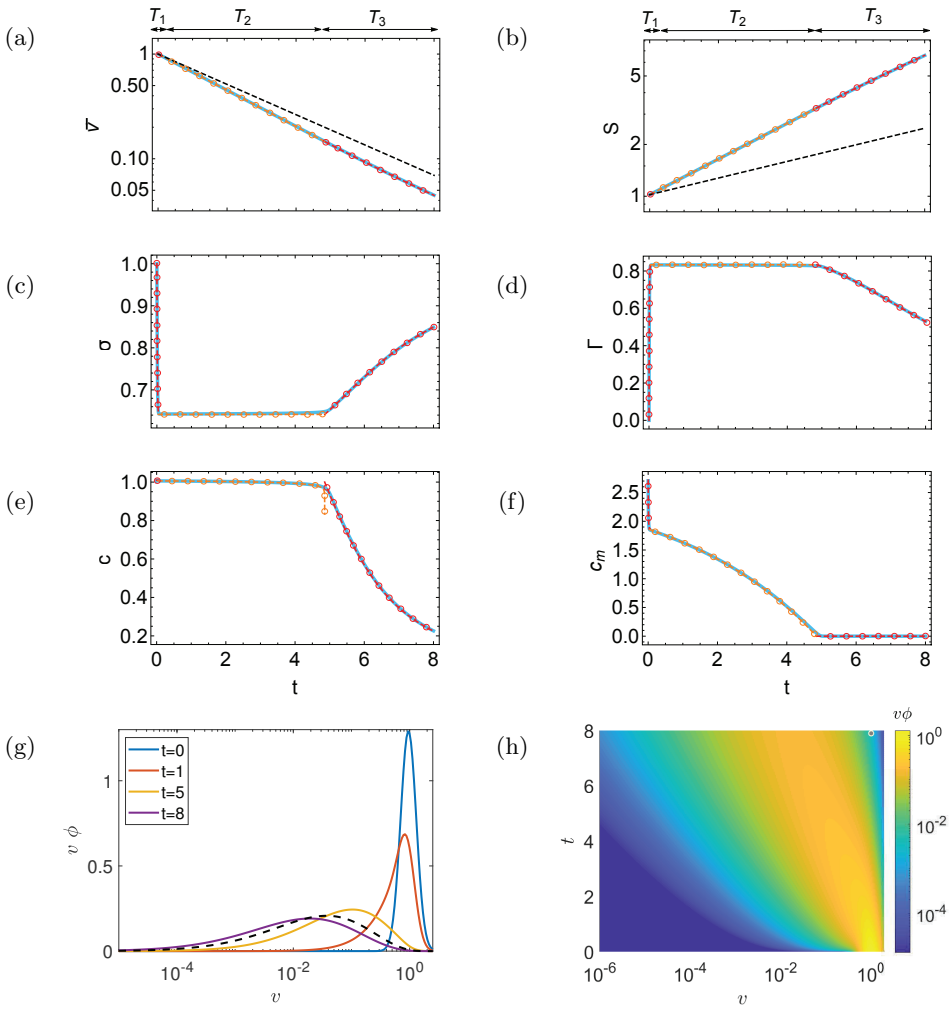

FIG. 2. *Solution of* (2.13)*, with uniform breakup rate* $\gamma = \sigma^{-2/5}$ *and parameter values* $\theta = 0.2$*,* $\eta = 0.2$*,* $\alpha = 1$*,* $\mathcal{K}_0 = \mathcal{K}_a = N_m = 10^2$*, and* $\mathcal{C}_0 = 3.7$*.* (a)–(f) *Solid blue curves show the numerical solution. The asymptotic solutions are shown using dashed curves and open circles: red for* T_1 *and* T_3*, orange for* T_2*. Black dashed lines in* (a) *and* (b) *show results* (4.9) *for no surfactant.* (a) *Average drop volume* $\bar{v}$*;* (b) *drop surface area* S*;* (c) *surface tension* σ*;* (d) *adsorbed surfactant concentration per unit area,* Γ*;* (e) *free monomer concentration* c*;* (f) *micelle concentration* c_m*.* (g) *Drop size distribution* $v\phi$ *plotted versus* $\log v$ *for various times* t*. Black dashed curve shows results for no surfactant at* $t = 8$*.* (h) *Variation of drop size distribution* $v\phi$ *with* $\log v$ *and* t*.*

If there is no surfactant in the system, then $\mathcal{C}_0 = 0$ so $c = c_m = \Gamma = 0$, and it follows that $\sigma = 1$ and the solution of the system (4.3), (4.4) is given by

$$\bar{v}(t) = \mathrm{e}^{-t/3}, \qquad S(t) = S(0)\mathrm{e}^{t/9}. \tag{4.9}$$

The mean drop size decreases exponentially and the droplet surface area correspondingly increases exponentially, as illustrated by the black dashed lines in Figure 2(a) and (b).

Now let us include the effect of surfactant. We take the illustrative parameter values $\theta = 0.2$, $\eta = 0.2$, $\alpha = 1$, $\mathcal{K}_0 = \mathcal{K}_a = N_m = 10^2$, and $\mathcal{C}_0 = 3.7$. The blue solid

curves in Figure 2(a)–(f) show numerical solutions of the ODE system (4.3)–(4.4). The solid lines in Figure 2(g) illustrate $v\phi$ versus $\log v$ for increasing values of t, from (4.8). Since $\phi\,\mathrm{d}v = v\phi\,\mathrm{d}(\log v)$, this choice of axes ensures that the area under the graph is conserved. Figure 2(h) is a surface plot of $v\phi$, in the $(\log v, t)$-plane.

With increasing time, as the drops break up, the mode of the distribution shifts toward smaller droplet sizes, and the distribution becomes more spread out. At large times, drops continue to break up and no steady state is reached. This behavior is a facet of the simple breakup model allowing small droplets to keep breaking up indefinitely; we will show in section 5 the effects of a more realistic model that limits the breakup of very small droplets. In Figure 2(g), we compare the distribution at $t = 8$ with that with no surfactant, in dashed black. Compared to the case with no surfactant, the distribution is focused on smaller drop sizes, as the decrease in surface tension has encouraged greater droplet breakup. However, we also see that the surface tension is not constant through the process; the surfactant concentrations evolve in response to the changes in droplet surface area.

Figure 2(a)–(f) show that the dynamics occurs over three distinct phases, labeled T_1–T_3. In the first (short-lived) phase, Γ rapidly increases and c_m decreases, as surfactant adsorbs to the droplet surfaces, thus depleting the supply of micelles in the bulk. During the second phase, Γ and c remain roughly constant, but, due to the increase in droplet surface area, the total fraction of adsorbed surfactant increases and the micelle concentration c_m decreases as a result. The third phase commences when the system has run out of micelles; then the bulk and surface concentration both start to decrease, so the surface tension increases and the rate of breakup slows down. We next analyze each of these phases using asymptotic analysis, based on the expected magnitude of the dimensionless rate constants $\mathcal{K}_0$, $\mathcal{K}_a$ and the micelle size N_m.

4.2. Asymptotic solution. We now explicitly assume that $\mathcal{K}_0$, $\mathcal{K}_a$, and N_m are all asymptotically large, while treating other parameters as $\mathcal{O}(1)$. The large rate constants mean that the system rapidly approaches a state of thermodynamic equilibrium, the evolution to which describes the first phase T_1. During the subsequent phases T_2 and T_3, the concentrations c, c_m, and Γ evolve quasi-steadily, slaved to the evolving droplet surface area S.

When $N_m \gg 1$, the term c^{N_m} in (4.3c) is exponentially small whenever $c < 1$ and can only be order unity when $c - 1 = \mathcal{O}\left(N_m^{-1}\right)$. It can therefore be approximated by

$$c^{N_m} \sim \begin{cases} 0, & c < 1, \\ \mathrm{e}^{N_m(c-1)}, & c \sim 1 + \mathcal{O}\left(N_m^{-1}\right). \end{cases} \tag{4.10}$$

The switch between these two cases, which correspond to being above or below the CMC, is what distinguishes the dynamics in phases T_2 (the second case) and T_3 (the first).

We assume that $\mathcal{C}_0 > 1$, so the initial concentration of surfactant added to the system is above the CMC. Then, from (4.4b) and (4.5), we deduce the asymptotic initial conditions

$$c(0) \sim 1 + N_m^{-1}\log(\mathcal{C}_0 - 1), \qquad c_m(0) \sim \mathcal{C}_0 - 1 \tag{4.11}$$

as $N_m \to \infty$.

4.2.1. Phase T_1. The first phase of the dynamics occurs when $t = \mathcal{O}\left(\mathcal{K}_a^{-1}\right)$, and the surface concentration rapidly increases from its initial value to come into

equilibrium with the bulk. Over this short time-scale, the average volume $\overline{v}$ and surface area S do not depart significantly from their initial values. So long as the concentration remains above the CMC, we can use the approximation $c \sim 1$ in (4.3b) to obtain the decoupled ODE

$$\frac{d\Gamma}{dt} \sim \mathcal{K}_a \left[1 - (1+\eta)\Gamma\right]. \tag{4.12}$$

The solution of (4.12) subject to $\Gamma(0) = 0$ is

$$\Gamma(t) \sim \frac{1}{1+\eta}\left[1 - \mathrm{e}^{-(1+\eta)\mathcal{K}_a t}\right], \tag{4.13a}$$

and the other variables are then given by

$$c_m(t) \sim \mathcal{C}_0 - 1 - \alpha S(0)\Gamma(t), \qquad \sigma(t) = 1 + \theta \log\bigl(1 - \Gamma(t)\bigr), \qquad c(t) \sim 1. \tag{4.13b}$$

The red dashed curves with open circles in Figure 2 demonstrate that (4.13) correctly captures the initial rapid adjustment of the concentrations to achieve equilibrium between the adsorbed and bulk surfactant phases.

The surface concentration Γ increases toward a maximum value $1/(1+\eta)$, and the micelle concentration c_m correspondingly decreases. Our supposition that the system remains above the CMC throughout phase T_1 is valid provided the initial concentration is sufficiently large, specifically

$$\mathcal{C}_0 > 1 + \frac{\alpha S(0)}{1+\eta}, \tag{4.14}$$

and we assume that this inequality is satisfied.

4.2.2. Phase T_2. At the end of phase T_1, the system has approached thermodynamic equilibrium and the surfactant evolution equations (4.3b), (4.3c) become quasi-steady. This means that, together with the conservation equation (4.4b), we have algebraic relations

$$\Gamma = \frac{c}{\eta + c}, \qquad c_m = c^{N_m}, \qquad \mathcal{C}_0 = c + \frac{\alpha c S}{\eta + c} + c^{N_m}. \tag{4.15}$$

During phase T_2, the system is still above the CMC, so $c \sim 1 + \mathcal{O}\left(N_m^{-1}\right)$ in (4.10). Using the quasi-steady algebraic equations (4.15), it just remains to solve one ODE (4.3a) for the average volume $\overline{v}$. We thus obtain the asymptotic solution in phase T_2 as

$$\overline{v}(t) \sim \mathrm{e}^{-\sigma_c^{-2/5} t/3}, \qquad c_m(t) \sim \mathcal{C}_0 - 1 - \frac{\alpha S(0)}{1+\eta}\,\mathrm{e}^{\sigma_c^{-2/5} t/5}, \tag{4.16a}$$

$$S(t) \sim S(0)\mathrm{e}^{\sigma_c^{-2/5} t/5}, \qquad c(t) \sim 1 + N_m^{-1} \log c_m(t), \tag{4.16b}$$

where σ_c is the approximately constant (minimum) value of surface tension, obtained

from the constant surface surfactant concentration $\Gamma \sim 1/(1+\eta)$, namely,

$$\sigma_c = 1 + \theta \log\left(\frac{\eta}{1+\eta}\right). \tag{4.16c}$$

The asymptotic solution (4.16) is shown by orange dashed curves and open circles in Figure 2(a)–(f). The surface concentration remains roughly constant, and the consequently reduced surface tension causes an increased breakup rate compared with the case with no-surfactant (shown by the black dashed curve in Figure 2(a)–(b)). The corresponding increase in surface area causes the concentration of available micelles in the bulk to decrease, reaching zero at a critical time

$$t = t_c \sim 5\sigma_c^{2/5} \log\left(\frac{(1+\eta)(\mathcal{C}_0 - 1)}{\alpha S(0)}\right). \tag{4.17}$$

4.2.3. Phase T_3. For $t > t_c$, we enter phase T_3. The system is still in thermodynamic equilibrium but now below the CMC, so the micelle concentration c_m is approximately zero. From (4.15), the monomer concentration is thus approximated by $c \sim \mathcal{C}_0 - \alpha S\Gamma$, and to leading order satisfies the quadratic equation

$$(\mathcal{C}_0 - c)\,(\eta + c) - \alpha S c = 0. \tag{4.18}$$

The larger root of (4.18) determines c as a function of the surface area S. Then (4.3a) and (4.4c) may be reformulated as a separable ODE for $S(t)$, namely,

$$\frac{dS}{dt} = \frac{S}{9}\left[1 - \theta \log\left(\frac{\eta + \mathcal{C}_0 - \alpha S + \sqrt{(\eta - \mathcal{C}_0 + \alpha S)^2 + 4\eta\mathcal{C}_0}}{2\eta}\right)\right]^{-2/5}, \tag{4.19a}$$

which is solved subject to

$$S(t_c) = (\mathcal{C}_0 - 1)(1+\eta)/\alpha. \tag{4.19b}$$

The solution of (4.19) gives an implicit transcendental equation for $S(t)$, and the other dependent variables are then determined in terms of S. The red dashed curves and open circles in the region marked T_3 in Figure 2(a)–(f) show that the behavior of the full averaged model is well captured by the asymptotics. Now the system is below the CMC, the bulk concentration c and surface concentration Γ gradually decrease, and the surface tension σ therefore returns toward its undisturbed value of 1. Ultimately, the system therefore reduces to the surfactant-free dynamics, with $\overline{v} \sim \text{const} \times \mathrm{e}^{-t/3}$ as $t \to \infty$, albeit with a smaller prefactor multiplying the exponential, as can be seen by comparison with the black dashed curve in Figure 2(a).

4.2.4. Influence of other parameters. In the simple averaged model analyzed above, the maximal rate of droplet breakup occurs during phase T_2, when the surface tension is approximately constant at its minimum value. The net droplet breakup can thus be increased by either decreasing the equilibrium surface tension σ_c or by increasing the duration t_c of phase T_2. The value of σ_c, as defined by (4.16c), depends only on characteristic properties of the surfactant being used, and in principle one should try to design the surfactant (in conjunction with other additives) to make σ_c as small as possible.

In the solution shown in Figure 2, we have set $\alpha = 1$ but, in practice, α may be quite small. A small value of α implies that only a small proportion of the available

surfactant is adsorbed at the droplet surfaces, and it therefore takes a long time for the surface area to become large enough to significantly deplete the bulk surfactant. As shown by (4.17), the duration of rapid breakup t_c grows logarithmically with α. In other respects, the dynamics for small α resembles the behavior seen in Figure 2.

5. Drop-size dependent breakup rate. In the previous section, because of the assumption that the breakup rate is independent of drop size, the model predicts that the mean drop size decreases to zero at large times. In reality, we expect surface tension effects to have an increasingly important influence, ultimately preventing breakup of the smallest droplets. This expectation is captured by the more complicated constitutive relation (3.5) for the breakup rate. In Figure 3, we show numerical solutions of the full model (2.13) using the breakup rate (3.5) and daughter drop distribution (3.7). These are obtained using the method of lines: drop size is discretized uniformly in $\log d$, with 400 bins, the trapezoidal rule is used to evaluate the volume integral in (2.13a), and the resulting system of ODEs is solved using ode15s in MATLAB. The method has been validated by using it to reproduce the semianalytical solutions found in section 4. Parameter values are taken to be $b = 0.5 \times 10^{-3}$, $\theta = 0.2$, $N_m = 20$, $\eta = \alpha = 1/\mathcal{K}_0 = 1/\mathcal{K}_a = 0.01$, and $\mathcal{C}_0 = 2.1$. Note the chosen parameter values now reflect the anticipated smallness of η and α.

Using the modified breakup rate produces qualitatively different results from those in Figure 2. The broad pattern of rapidly decreased surface tension (and therefore increased breakup) followed by gradual recovery once the micelle concentration is depleted is similar. However, the significant difference is the presence of the Heaviside function in (3.5), which prevents droplets below a critical size from breaking up and results in convergence to a steady-state distribution, rather than the continual breakup that occurs in Figure 2.

At very small times (corresponding to phase T_1 from subsection 4.2), the surface concentration Γ reaches approximate equilibrium with the bulk. During phase T_2 (for $t \lesssim 8$ in this case), the system remains above the CMC and the bulk concentration c therefore remains almost constant. Droplet breakup causes a large increase in the surface area S, by around two orders of magnitude, and the resulting dilution of the adsorbed surfactant in turn causes a slight dip in Γ, which translates to a noticeable increase in σ. As the increase in S levels off, Γ starts to increase again as the system returns to thermodynamic equilibrium, and σ, in turn, decreases. Finally, for $t \gtrsim 8$, the system drops below the CMC and we enter phase T_3 of the dynamics, during which the bulk concentration c falls to close to zero. Unlike in section 4, droplet breakup eventually slows and then stops, and S approaches a steady state value by around $t \approx 35$. Since the droplet surface area does not keep increasing, the absorbed surface concentration is no longer being diluted and so Γ reaches a nonzero constant equilibrium value.

The volume distribution $\phi(v, t)$ is initially localized around $v = 1$. As the larger drops break up, this local peak diminishes and moves to the left, and a large volume fraction of smaller droplets is produced. According to the breakup function (3.5), instead of breaking up indefinitely, the smaller droplets cluster around the critical minimum droplet size $v_c = (b\sigma)^{9/5}$, which evolves in time according to the surface tension σ. At intermediate times (see, e.g., $t = 5$), the distribution becomes bimodal, with local maxima close to both the initial mean volume $\overline{v}(0) = 1$ and the critical volume v_c at this time. The critical volume v_c depends on σ and therefore increases for $t \gtrsim 8$, resulting in the formation of a new peak in the distribution function, which again becomes bimodal for $t \gtrsim 8$. At large times, for $t \gtrsim 20$, as droplet breakup

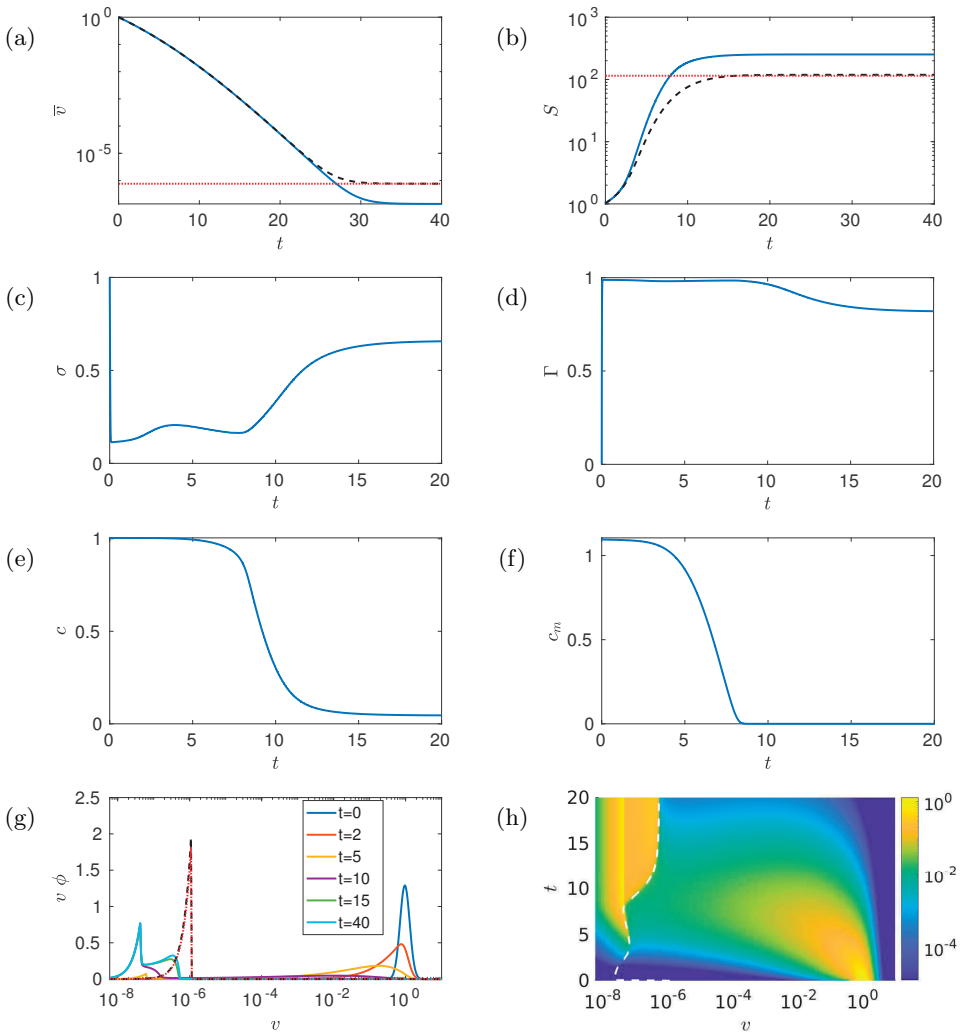

FIG. 3. *Numerical solutions of full-distribution model* (2.13) *using breakup rate* (3.5) *and daughter drop distribution* (3.7)*, with parameter values* $b = 0.5 \times 10^{-3}$*,* $\theta = 0.2$*,* $N_m = 20$*,* $\eta = \alpha = 1/\mathcal{K}_0 = 1/\mathcal{K}_a = 10^{-2}$*, and* $\mathcal{C}_0 = 2.1$*.* (a)–(f) *Mean drop volume* $\overline{v}$*, surface area* S*, surface tension* σ*, adsorbed surfactant concentration* Γ*, free monomer concentration* c*, and micelle concentration* c_m *versus time* t*. Black dashed curves show results for no surfactant. Note the different scaling of the horizontal axis in* (a)–(b)*.* (g) *Drop size distribution* $v\phi$ *plotted versus* $\log v$ *for increasing values of time* t*. Black dashed curve shows results for no surfactant at* $t = 20$*.* (h) *Variation of drop size distribution* $v\phi$ *with* $\log v$ *and* t*. The white dotted curve is* $v_c(t) = (b\sigma(t))^{9/5}$*, the critical drop size below which no drops break up. In* (a)*,* (b)*, and* (f) *the red dotted curves are the final state mean drop size, surface area, and drop size distribution, respectively, for the case with no surfactant given by* (5.4)–(5.5)*.*

slows, the system converges to a steady state. Eventually, by around $t \approx 35$, all of the droplets which could have broken up have done so and a steady-state distribution is reached with $\phi(v,t) \equiv 0$ for $v > v_c$.

In Figure 3(g), the steady-state distribution at $t = 20$ when no surfactant is added is plotted as a black dashed curve. Here the critical size v_c, below which no drops break up, is larger and is fixed (since the surface tension is constant). Thus

the distribution is unimodal, with its mode at the critical droplet size. Overall, the addition of surfactant has a significant impact on reducing the maximum droplet size and increasing the proportion of smaller droplets.

When using the breakup rate (3.5), since $\gamma(v) \equiv 0$ for $v < v_c(t)$, the evolution equation (2.13a) for ϕ reduces to

$$\frac{\partial \phi}{\partial t}(v,t) = \int_{v_c(t)}^{\infty} \gamma(\tilde{v},\sigma)\chi(v,\tilde{v})\phi(\tilde{v},t)\,\mathrm{d}\tilde{v} \tag{5.1}$$

for all $v < v_c(t)$. The only v-dependence in the right-hand side arises from $\chi(v,\tilde{v})$, and the form of the daughter distribution function χ therefore controls the behavior of smaller droplets. Given the uniform daughter size distribution (3.7), (5.1) takes the form

$$\frac{\partial \phi}{\partial t}(v,t) = 2v \int_{v_c(t)}^{\infty} \frac{\gamma(\tilde{v},\sigma)}{\tilde{v}^2}\phi(\tilde{v},t)\,\mathrm{d}\tilde{v}, \tag{5.2}$$

so the rate of volume production increases linearly with v, and the largest proportion of drops is produced close to $v = v_c$.

In the case where no surfactant is added, the critical droplet size $v_c = b^{9/5}$ is constant and small. Ultimately, all of the droplets bigger than v_c break up, so the system approaches a final distribution in which

$$\phi(v,t) \to \phi_f(v) = \begin{cases} \phi_0(v) + Av, & v < v_c, \\ 0, & v > v_c, \end{cases} \quad \text{as } t \to \infty, \tag{5.3}$$

for some constant A. Since the tail of the initial distribution (2.15) is negligible for $v < v_c$ (with $b = 0.5 \times 10^{-3}$, we have $\phi_0(v) < 10^{-417}$ when $v < b^{9/5}$), the steady distribution may be found using mass conservation as

$$\phi_f(v) \sim \frac{2v\mathcal{H}(v_c - v)}{v_c^2}. \tag{5.4}$$

This final state does not depend on the form of the breakup rate γ except through the critical droplet size v_c. The final mean droplet size and surface area are, correspondingly, given by

$$\overline{v} = \frac{2v_c}{3}, \qquad S = \frac{6}{5v_c^{1/3}}. \tag{5.5}$$

We see in Figure 3(a), (b), and (g) that the numerical solutions converge to these values at larger times.

In the case where surfactant is added, the steady state distribution cannot be so easily determined, since v_c varies with time. However, we can confidently predict that the system ultimately does reach a steady state, with a nonzero surfactant concentration c and corresponding equilibrium surface tension given by

$$\sigma = 1 + \theta \log\left(\frac{\eta}{\eta + c}\right). \tag{5.6}$$

Since all of the drops must end up being smaller than the final critical size $v_c = (b\sigma)^{9/5}$, we can write the final surface area as

$$S = \frac{1}{\xi v_c^{1/3}}, \tag{5.7}$$

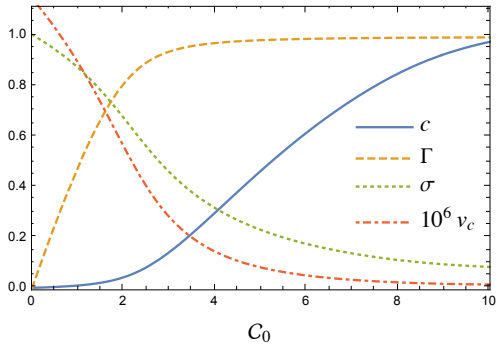

FIG. 4. *Estimates for the final monomer concentration c, adsorbed surface concentration Γ, surface tension σ, and (scaled) critical volume v_c, plotted versus the total surfactant concentration $\mathcal{C}_0$. These estimates are obtained by using the approximation* (5.8)*, with $\xi = 0.5$ and other parameter values as in Figure* 3.

where $\xi \in (0, 1)$ parameterizes how much the distribution spreads below the critical volume v_c. The total surfactant conservation law (2.13g) thus provides a nonlinear algebraic equation relating c to $\mathcal{C}_0$ and ξ, namely,

$$\mathcal{C}_0 = c + c^{N_m} + \frac{\alpha}{\xi b^{3/5}} \frac{c}{\eta + c} \left[1 + \theta \log\left(\frac{\eta}{\eta + c} \right) \right]^{-3/5}. \tag{5.8}$$

The spread of the final distribution below $v = v_c$ cannot be determined a priori without solving for the entire evolution of the system. Nevertheless, with ξ an order-one parameter, (5.8) gives at least a qualitative relation between the input surfactant concentration $\mathcal{C}_0$ and the final bulk concentration c. Moreover, armed with our estimate for c, we can then compute estimates of the remaining key quantities. If we take a representative value of $\xi = 0.5$, then, using the parameter values from Figure 3, we find the approximate relations between $\mathcal{C}_0$ and monomer concentration c, adsorbed surface concentration Γ, surface tension σ, and critical volume v_c depicted in Figure 4. With $\xi = 0.5$, we obtain $c \approx 0.048$ from (5.8), and then approximate the surface area and surface concentration as $S \approx 248$ and $\Gamma \approx 0.83$, which are all encouragingly in line with the numerically computed values of $c = 0.0353$, $S = 266.3$, and $\Gamma = 0.78$ observed in Figure 3. Although ad hoc, such approximations can provide useful rules of thumb for practitioners to determine how much surfactant must be added to achieve desired values of these quantities at the end of the process. It is noteworthy that the approximation (5.8) does not depend on the details of the droplet breakup law: it relies only on the existence of a critical droplet size that scales self-consistently with the surface tension, as well as a plausible guess for the parameter ξ.

6. Different surfactant injection scenarios.

6.1. Varying surfactant concentration. We have shown that our model captures the interaction between adsorbed surfactant and dissolved monomers and micelles and how the resulting reduction in surface tension promotes droplet breakup. We will now use the model to investigate how the amount of surfactant used and the way in which it is added influence the net effectiveness of droplet breakup. It is useful to construct a metric to compare the effectiveness of different surfactant injection protocols. In practice, the aim is to ensure that as large a fraction of oil as possible is in droplets small enough so they can disperse in the water. Therefore, we calculate

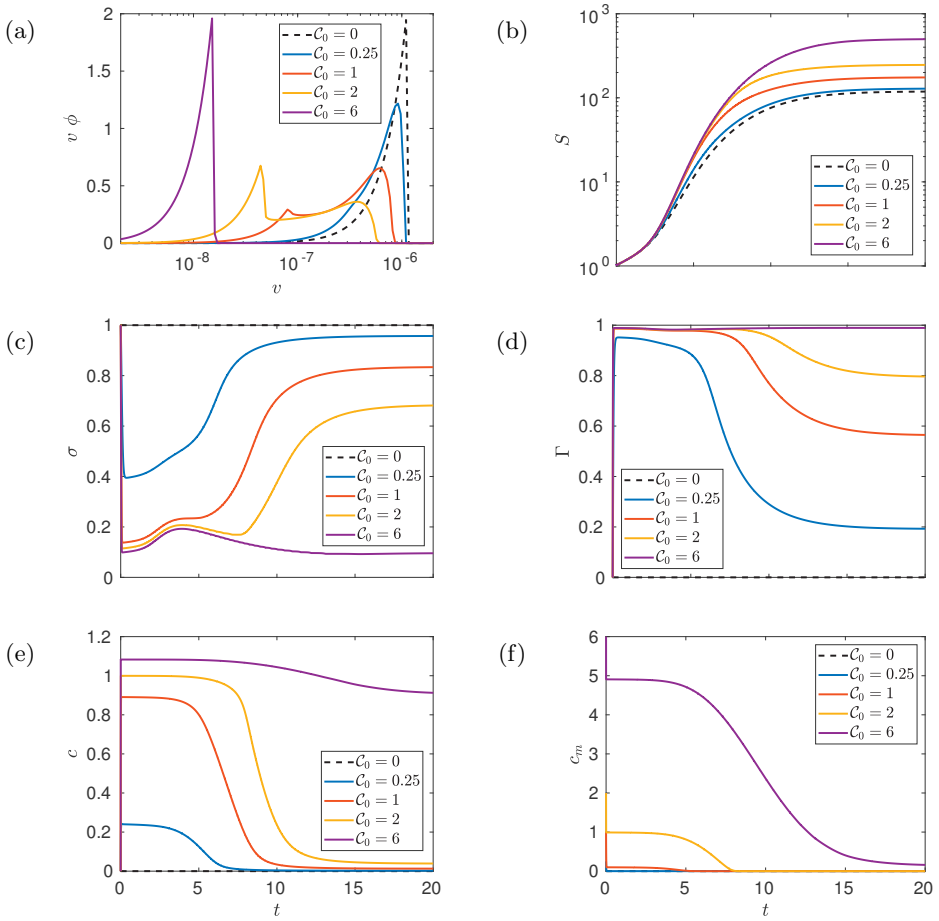

FIG. 5. *Numerical solutions of full-distribution model* (2.13) *using breakup rate* (3.5) *and daughter drop distribution* (3.7), *with parameter values* $b = 0.5 \times 10^{-3}$, $\eta = \alpha = 1/\mathcal{K}_0 = 1/\mathcal{K}_a = 10^{-2}$, $N_m = 20$, $\theta = 0.2$ *and different values of the added surfactant concentration* $\mathcal{C}_0$. (a) *Final drop size distribution at* $t = 50$, $v\phi$ *plotted versus* $\log v$; (b)–(f) *surface area* S, *surface tension* σ, *adsorbed surfactant concentration* Γ, *free monomer concentration* c, *and micelle concentration* c_m *versus time* t. *Black dashed curves show results for no surfactant.*

the fraction f_d of droplets below a certain diameter d, that is,

$$f_d(t) = \int_0^{\pi d^3/6} \phi(v,t)\,\mathrm{d}v, \tag{6.1}$$

with d here taken to be 0.005.

First we consider the effect of varying the total concentration $\mathcal{C}_0$ of surfactant in the system. In Figure 5, we show numerical solutions of the full model (2.13) using breakup rate (3.5) and daughter drop distribution (3.7), with different values of $\mathcal{C}_0$ and all other parameter values the same as in Figure 3.

When $0 < \mathcal{C}_0 \lesssim 1$, the added surfactant is below the CMC so there is no store of micelles to keep the available surfactant topped up. The surface tension decreases initially, but recovers relatively soon toward values close to the undisturbed value as the surfactant is adsorbed onto the increasing surface area of the drops. The eventual

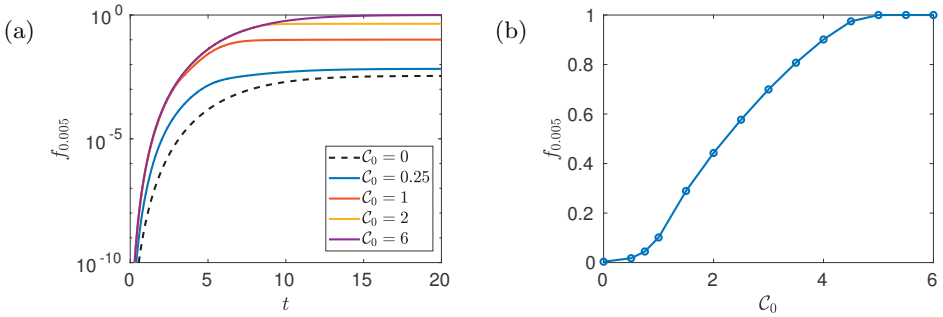

FIG. 6. *Fraction of drops with diameter $d < 0.005$* (a) *plotted versus time t for different concentrations $\mathcal{C}_0$ of injected surfactant and* (b) *versus $\mathcal{C}_0$ at final time $t = 50$. The same parameter values as Figure 5 are used here.*

steady distribution shown in Figure 5(a) therefore varies only marginally from the no-surfactant case $\mathcal{C}_0 = 0$. The case with $\mathcal{C}_0 = 2$ is qualitatively similar to the solution shown in Figure 3. There is a significant phase T_2, during which the system remains above the CMC and the surface concentration Γ is close to 1, following which the system converges to a steady state with $\Gamma \approx 0.6$. The steady distribution is bimodal, with two local maxima reflecting the two associated values of the cut-off droplet volume v_c. When a large concentration $\mathcal{C}_0 = 6$ is added, the micelles never run out (i.e., the system never enters phase T_3) and so the surface concentration Γ remains high while the drops are breaking up, resulting in a unimodal steady distribution. The dynamics is essentially equivalent to that for a constant, but lower, value of surface tension and therefore a smaller final critical drop size v_c.

Figure 6(a) shows how the fraction $f_{0.005}$ of droplets below our chosen dimensionless diameter $d = 0.005$ varies with time for each of the values of $\mathcal{C}_0$ used in Figure 5. In Figure 6(b), we plot the eventual steady-state value of the fraction $f_{0.005}$ of small droplets versus the injected surfactant concentration $\mathcal{C}_0$. With $\mathcal{C}_0 \lesssim 1$, the fraction of small droplets departs only marginally from the no-surfactant case $\mathcal{C}_0 = 0$. As the added surfactant concentration increases above the CMC ($\mathcal{C}_0 \gtrsim 1$), there is a significant increase in the fraction of small droplets with $d < 0.005$. Adding more surfactant initially serves to increase the micelle concentration but, with time, these additional micelles disassociate and further reduce the surface tension, leading to the production of small droplets. Above a critical concentration $\mathcal{C}_0 \approx 5.5$, all of the droplets ultimately end up below the target diameter $d = 0.005$. Any additional surfactant goes into creating unnecessarily smaller droplets.

We can use (5.6) and (5.8) to estimate the critical surfactant concentration required to ensure that *all* of the droplets end up smaller than a given diameter d. Setting $v_c = (b\sigma)^{9/5} = \pi d^3/6$, we find from (5.6) that the corresponding value of the bulk monomer concentration is

$$c = \eta \left\{ \exp\left[\frac{1}{\theta} \left(1 - \frac{1}{b} \left(\frac{\pi d^3}{6} \right)^{5/9} \right) \right] - 1 \right\} \approx 0.525 \tag{6.2}$$

with the parameter values used in Figure 5. We then infer from (5.8) (persisting with the postulated value of $\xi = 0.5$) a critical total concentration of $\mathcal{C}_0 \approx 5.4$, which is nicely in line with what we observe in Figure 6(b).

6.2. Varying surfactant injection method. We have thus far assumed that all the available surfactant is added to the system at $t = 0$. We now relax this assumption and model the effects of different injection methods by taking $C(t)$ not to be a constant value $\mathcal{C}_0$ but instead to be an increasing function of t with maximum value $\mathcal{C}_0$. The bulk surfactant conservation equation (2.13d) is then modified to

$$\frac{dc}{dt} = -\mathcal{K}_0\left[c^{N_m} - c_m\right] - \mathcal{K}_a\alpha\left[(1-\Gamma)cS - \eta\Gamma S\right] + g(t) \tag{6.3}$$

with $c(0) = 0$, where

$$\frac{dC}{dt} = g(t) \tag{6.4}$$

is the net rate at which surfactant is added to the system.

We investigate here an idealized scenario in which the surfactant is injected at a constant rate over a time interval T, after which the net concentration stays at the constant value $\mathcal{C}_0$, i.e.,

$$C = \begin{cases} \mathcal{C}_0 t/T, & 0 \le t < T, \\ \mathcal{C}_0, & t \ge T. \end{cases} \tag{6.5}$$

The case we have considered thus far, where all the surfactant is injected instantaneously at $t = 0$, corresponds to the limit $T \to 0$, while larger values of T correspond to a more gradual addition of surfactant.

In Figures 7 and 8 we show results from numerical solutions of the full model (2.13) with the modified conservation equation (6.3). We use the size-dependent breakup rate (3.5) and uniform daughter drop distribution (3.7), with parameter values $b = 0.5 \times 10^{-3}$, $\theta = 0.2$, $N_m = 20$, $\eta = \alpha = 1/\mathcal{K}_0 = 1/\mathcal{K}_a = 10^{-2}$, and $\mathcal{C}_0 = 3$. We see that holding some surfactant in reserve and adding it gradually allows us to lower the value of the surface tension σ at large times, but means that we no longer achieve such small values of σ at small times.

When the surfactant is added rapidly, as in the $T = 0$ and $T = 10$ curves in Figure 7(a), we observe a bimodal distribution of droplet sizes, with very small droplets created during the early phase when the surface tension is very low, and larger droplets created later on. In contrast, larger values of T result in a unimodal distribution, with the droplet sizes more concentrated about the final critical maximum volume v_c. In terms of the discussion leading to (5.8), the stronger localization near $v = v_c$ corresponds to a larger value of ξ closer to 1, resulting in a larger final bulk concentration c for a given net concentration $\mathcal{C}_0$. The stronger focusing of the size distribution is ultimately responsible for a lower value of the final surface tension and therefore a smaller critical drop size v_c, as may be observed with $T \gtrsim 15$ in Figure 7(a).

Figure 8(a) shows the time evolution of the fraction f_d of droplets smaller than a critical dimensionless diameter d, here taken to be 0.004. Since the production of very small droplets occurs mainly over the time interval $t \lesssim 10$, the key to maximizing the proportion of small drops is to maximize the surfactant concentration during this initial period, when the surface area S is still relatively small. It follows that adding surfactant more slowly, i.e., increasing T in (6.5), always results in fewer of the smallest drops being produced.

In Figure 8(b), we show the evolution of f_d with a larger critical droplet size $d = 0.007$. In this case we achieve better results by introducing the surfactant more

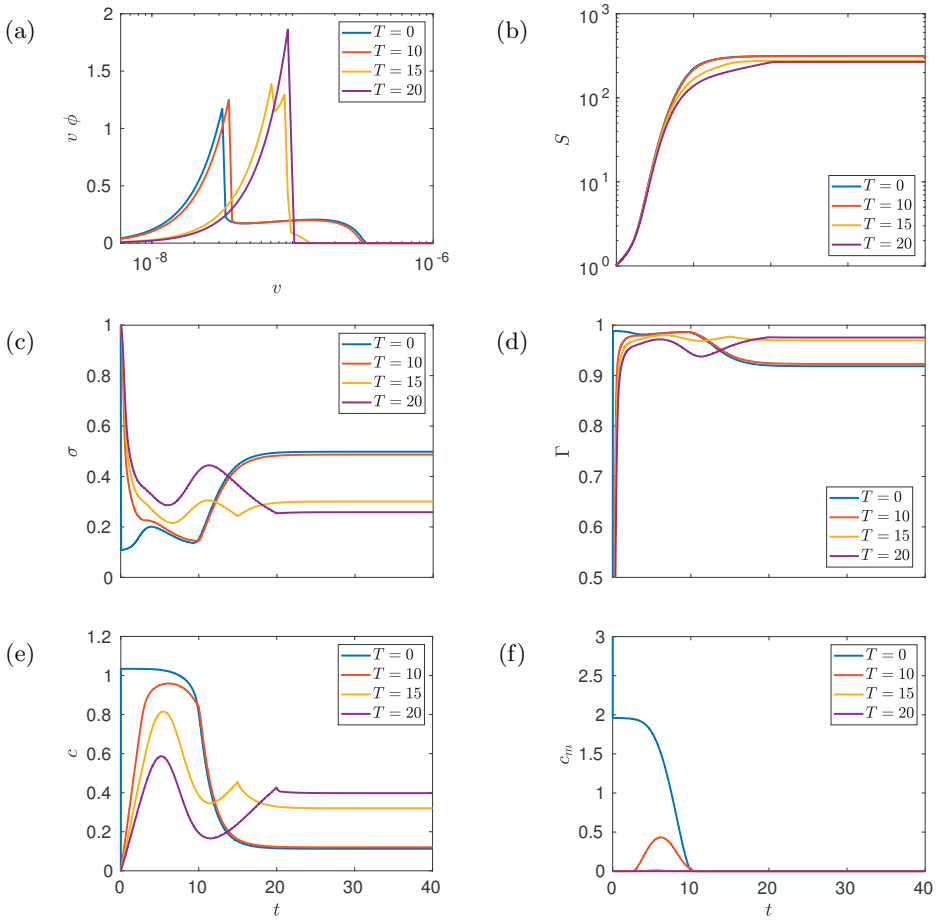

FIG. 7. *Numerical solutions of full-distribution model* (2.13) *using breakup rate* (3.5) *and daughter drop distribution* (3.7)*, with parameter values* $b = 0.5 \times 10^{-3}$*,* $\theta = 0.2$*,* $N_m = 20$*, and* $\eta = \alpha = 1/\mathcal{K}_0 = 1/\mathcal{K}_a = 10^{-2}$*. The surfactant is injected according to* (6.5) *with* $\mathcal{C}_0 = 3$ *and different values of the injection time* T*.* (a) *Steady-state drop size distribution,* $v\phi$ *plotted versus* $\log v$*;* (b)–(f) *surface area* S*, surface tension* σ*, adsorbed surfactant concentration* Γ*, free monomer concentration* c*, and micelle concentration* c_m *versus time* t*.*

gradually: all of the droplets with a diameter larger than d are eventually eliminated only for the largest values of $T = 15$ or 20. This figure demonstrates that, when the total quantity of available surfactant is limited, improved performance may be gained by adding the surfactant intelligently. Keeping the surface tension roughly constant during droplet breakup results in a localized final distribution with a smaller value of v_c for a given $\mathcal{C}_0$. In contrast, when we add the surfactant all at once, we create a lot of very small droplets early on, thereby depleting the available surfactant and ultimately leaving a significant tail of larger droplets that never break up.

Figure 8(c) demonstrates how the optimum surfactant injection strategy depends on the target droplet diameter d. Given the total surfactant concentration $\mathcal{C}_0 = 3$, it is impossible to make all of the droplets smaller than the smallest size $d = 0.004$; the best strategy in this case is to add all of the surfactant at the start to generate as many small droplets as possible. However, for larger values of d, one can increase the

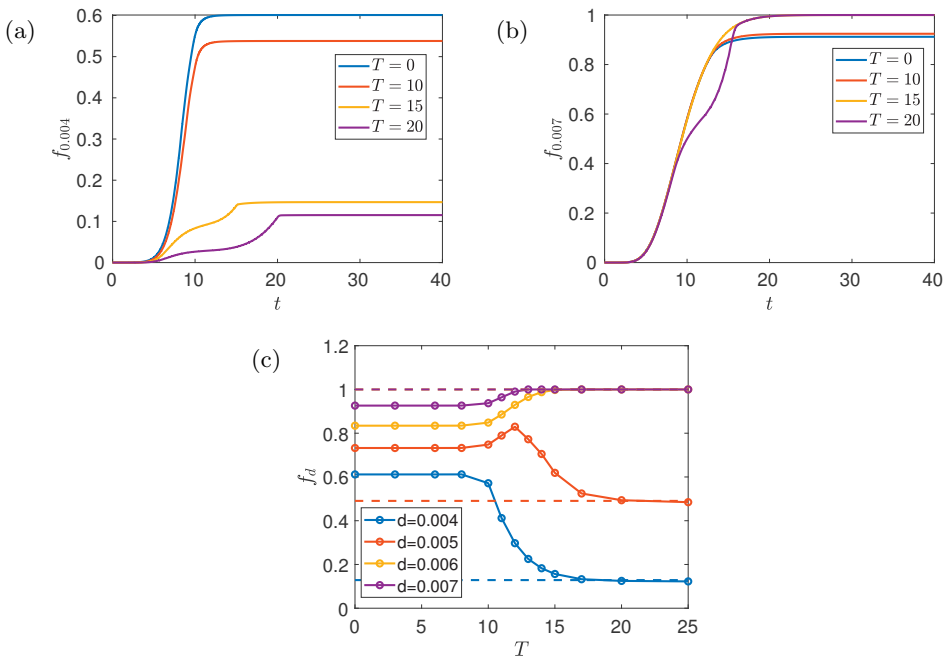

FIG. 8. *Fraction f_d of droplets with diameter smaller than* (a) $d = 0.004$ *and* (b) $d = 0.007$, *versus time t, with the same parameter values as in Figure 7.* (c) *Fraction f_d versus T for different d. Large T approximation* (6.7) *in dashed lines. Note for simulations in* (c) *we discretize uniformly in* $\log d$, *with* 600 *bins.*

value of f_d by introducing the surfactant gradually. With $d = 0.005$ and $d = 0.006$, there is an optimum choice of time-scale T that produces the greatest fraction of small droplets. For the largest value of $d = 0.007$, the fraction f_d of small droplets increases monotonically with T, and one can entirely eliminate droplets with a larger diameter than 0.007 if T is taken sufficiently large.

In the limit of extremely slow addition of surfactant, with $T \gg 1$, the system must evolve quasi-steadily through a sequence of equilibrium states parameterized by the value of the total surfactant concentration $C(t)$. Provided $C(t)$ is monotonically increasing, we expect the surface tension σ, and therefore also the critical droplet volume v_c, to be monotonically decreasing functions of t. The minimum value of v_c is therefore attained in the limit $t \to \infty$, and ultimately, when all of the droplets larger than v_c have broken up, the distribution must approach the piecewise linear function $\phi_f(v)$ given by (5.4). We deduce that the final bulk concentration c and the total injected surfactant concentration $\mathcal{C}_0$ satisfy the relation (5.8) with $\xi = 5/6$. The droplet size distribution is then exactly the same as (5.4) (for the case where no surfactant is added), namely,

$$\phi \sim \frac{2v\mathcal{H}(v_c - v)}{v_c^2}, \tag{6.6}$$

just with a smaller constant value of the surface tension and so a smaller value of v_c. For the case where $T = 20$, this is approximately true, with ϕ in Figure 7(a) approximately proportional to v for $v < v_c$.

With $\xi = 5/6$ and the other parameter values as in Figures 7 and 8, we find from (5.8) that the final bulk concentration is given by $c \approx 0.4177$, and the corresponding

values of the surface tension and critical droplet volume are $\sigma \approx 0.2488$ and $v_c \approx 9.348 \times 10^{-8}$. Using this value of v_c and inserting (6.6) into (6.1), it follows that, in the limit where T is very large, the fraction of droplets smaller than a given diameter d approximately takes the form

$$f_d \sim \begin{cases} \left(\frac{d}{d_c}\right)^6, & d < d_c, \\ 1, & d \geq d_c, \end{cases} \tag{6.7}$$

with $d_c \approx 0.00563$. The case where $T = 20$ approaches this large T approximation, as shown by the dashed lines in Figure 8(c).

7. Discussion and conclusions. In this paper, we have constructed a mathematical model for the breakup of oil droplets in a homogeneous turbulent flow and used the model to examine how the droplet size distribution varies with surfactant application. The large-time behavior of the system is of most interest and, as we have shown, is highly dependent on the choice of constitutive relation for the droplet breakup rate. If droplets of all sizes are allowed to keep breaking up (as in section 4), there is no steady state. The surface tension eventually returns to its undisturbed value, and so the late-time behavior is similar to that with no surfactant.

It is more realistic to impose a constitutive relation that limits the breakup of very small droplets (as in section 5). In this case, the breakup dynamics separates into two distinct phases (T_2 and T_3) corresponding to the bulk surfactant concentration being above or below the CMC. In the first of these phases the surface tension is essentially determined by the equilibrium surfactant properties. At later times, the surface tension tends toward a constant value that is not necessarily equal to the undisturbed value, but depends on the history of the drop-surfactant interaction, and in particular on the amount of droplet surface area that has been created. Such subtleties cannot be captured by just changing the undisturbed surface tension to a new lower constant value, as has been done in similar population models used previously in the literature [25, 24].

Our model enables us to examine how to optimize surfactant application. We find, unsurprisingly, that increasing the total surfactant concentration $\mathcal{C}_0$ facilitates the production of smaller droplets. Equation (5.8) allows one to estimate how the final values of the surfactant concentration and maximum droplet size depend on $\mathcal{C}_0$, in terms of an order-one dimensionless parameter ξ that characterizes the spread of the droplet size distribution. For a given value of $\mathcal{C}_0$, one can reduce the maximum remaining droplet size by achieving a more localized distribution and thus increasing the value of ξ. Consequently, it can be advantageous to add the surfactant gradually, in such a way as to keep the surface tension approximately constant, and thereby produce droplets that are all of a similar size. In contrast, adding all of the surfactant at once tends to produce a bimodal distribution, dominated by both very small and medium-sized droplets.

Our model makes a number of simplifying assumptions. First, while we focus on droplet breakup, we neglect coalescence. This is a reasonable assumption for relatively small volume fractions of droplets, so that droplet-droplet collisions occur infrequently. Moreover, when droplets are coated with surfactant, they may be less likely to coalesce even if they come into contact. Second, we assume that Γ is the same for all droplets. If the system is not in thermodynamic equilibrium, when a larger drop breaks into two smaller droplets the value of Γ on the daughter droplets changes. An alternative model might take ϕ to be a distribution over both v and Γ. However, after the short

and uninteresting stage T_1, the system is close to thermodynamic equilibrium, and it is therefore reasonable to take Γ to be the same for all droplets, at least during stages T_2 and T_3 when significant breakup occurs.

In addition, our results rely on our choice of constitutive law (3.5) for the droplet breakup rate. More complex breakup rates may be found, e.g., in [23, 24, 25, 26], which draw an analogy between the interaction of droplets with the deforming turbulent eddies and collisions in ideal gases. There are various other competing theories but it is difficult to ascertain which of these is correct [15], since the droplet breakup cannot be measured directly in experiments. Instead, a particular breakup rate can only be validated by using a droplet population model to predict drop size distribution for comparison with empirical data. Simpler breakup rates, such as that used in (3.5), make no attempt to capture secondary droplet phenomena such as tip-streaming, where turbulent shearing produces long thin trails of oil behind a drop [11]. However, they incorporate the important large-scale features of droplet breakup and can be more directly validated with experimental data, as in [17].

In principle, it is not difficult to extend our model to include spatial variation as well as time evolution. This is useful in examining what happens in a deep-sea oil spill, for example, where a turbulent jet of oil is released from the ocean floor. The breakup of oil drops in this turbulent flow and the effect of surfactants can then be coupled to models for the motion and energy of the turbulent jet, with the added complications of transport and dilution, which mean that Φ and C are no longer conserved quantities [20].

REFERENCES

[1] R. G. Alargova, I. I. Kochijashky, M. L. Sierra, and R. Zana, *Micelle aggregation numbers of surfactants in aqueous solutions: A comparison between the results from steady-state and time-resolved fluorescence quenching*, Langmuir, 14 (1998), pp. 5412–5418, https://doi.org/10.1021/la980565x.

[2] P. J. Brandvik, Ø. Johansen, F. Leirvik, U. Farooq, and P. S. Daling, *Droplet breakup in subsurface oil releases–Part* 1: *Experimental study of droplet breakup and effectiveness of dispersant injection*, Marine Pollut. Bull., 73 (2013), pp. 319–326, https://doi.org/10.1016/j.marpolbul.2013.05.020.

[3] C. J. W. Breward, I. M. Griffiths, P. D. Howell, and C. E. Morgan, *Straining flow of a weakly interacting polymer–Surfactant solution*, European J. Appl. Math., 26 (2015), pp. 743–772, https://doi.org/10.1017/S0956792515000327.

[4] C. J. W. Breward and P. D. Howell, *Straining flow of a micellar surfactant solution*, European J. Appl. Math., 15 (2004), pp. 511–531, https://doi.org/10.1017/S0956792504005637.

[5] R. V. Calabrese, T. P. K. Chang, and P. T. Dang, *Drop breakup in turbulent stirred-tank contactors. Part* I: *Effect of dispersed-phase viscosity*, Amer. Inst. Chem. Eng. J., 32 (1986), pp. 657–666, https://doi.org/10.1002/aic.690320416.

[6] C.-H. Chang and E. I. Franses, *Adsorption dynamics of surfactants at the air/water interface: A critical review of mathematical models, data, and mechanisms*, Colloids Surfaces A, 100 (1995), pp. 1–45, https://doi.org/10.1016/0927-7757(94)03061-4.

[7] C. A. Coulaloglou and L. L. Tavlarides, *Description of interaction processes in agitated liquid-liquid dispersions*, Chem. Eng. Sci., 32 (1977), pp. 1289–1297, https://doi.org/10.1016/0009-2509(77)85023-9.

[8] P. Davidson, *Turbulence: An Introduction for Scientists and Engineers*, Oxford University Press, Oxford, 2015.

[9] Y. Fan, Y. Li, G. Yuan, Y. Wang, J. Wang, C. C. Han, H. Yan, Z. Li, and R. K. Thomas, *Comparative studies on the micellization of sodium bis (4-phenylbutyl) sulfosuccinate and sodium bis (2-ethylhexyl) sulfosuccinate and their interaction with hydrophobically modified poly (acrylamide)*, Langmuir, 21 (2005), pp. 3814–3820, https://doi.org/10.1021/la047129x.

[10] S. Friberg, K. Larsson, and J. Sjoblom, *Food Emulsions*, CRC Press, Boca Raton, FL, 2003.

[11] B. Gopalan and J. Katz, *Turbulent shearing of crude oil mixed with dispersants generates long microthreads and microdroplets*, Phys. Rev. Lett., 104 (2010), 054501, https://doi.org/10.1103/PhysRevLett.104.054501.

[12] J. O. Hinze, *Fundamentals of the hydrodynamic mechanism of splitting in dispersion processes*, Amer. Inst. Chem. Eng. J., 1 (1955), pp. 289–295, https://doi.org/10.1002/aic.690010303.

[13] Ø. Johansen, P. J. Brandvik, and U. Farooq, *Droplet breakup in subsea oil releases–Part 2: Predictions of droplet size distributions with and without injection of chemical dispersants*, Marine Pollut. Bull., 73 (2013), pp. 327–335, https://doi.org/10.1016/j.marpolbul.2013.04.012.

[14] A. Koshy, T. R. Das, and R. Kumar, *Effect of surfactants on drop breakage in turbulent liquid dispersions*, Chem. Eng. Sci., 43 (1988), pp. 649–654, https://doi.org/10.1016/0009-2509(88)87023-4.

[15] Y. Liao and D. Lucas, *A literature review of theoretical models for drop and bubble breakup in turbulent dispersions*, Chem. Eng. Sci., 64 (2009), pp. 3389–3406, https://doi.org/10.1016/j.ces.2009.04.026.

[16] C. Martínez-Bazán, J. L. Montanes, and J. C. Lasheras, *On the breakup of an air bubble injected into a fully developed turbulent flow. Part 1. Breakup frequency*, J. Fluid Mech., 401 (1999), pp. 157–182, https://doi.org/10.1017/S0022112099006680.

[17] C. Martínez-Bazán, J. L. Montanes, and J. C. Lasheras, *On the breakup of an air bubble injected into a fully developed turbulent flow. Part 2. Size PDF of the resulting daughter bubbles*, J. Fluid Mech., 401 (1999), pp. 183–207, https://doi.org/10.1017/S0022112099006692.

[18] S. P. Moulik and K. Mukherjee, *On the versatile surfactant Aerosol-OT (AOT): Its physicochemical and surface chemical behaviours and uses*, Proc. Indian Nat. Sci. Acad., 62 (1996), pp. 215–236.

[19] F. Peters and D. Arabali, *Interfacial tension between oil and water measured with a modified contour method*, Colloids and Surfaces A, 426 (2013), pp. 1–5, https://doi.org/10.1016/j.colsurfa.2013.03.010.

[20] R. Philip, *Modelling the Breakup of Droplets in a Turbulent Jet*, University of Oxford, Oxford, UK, 2018.

[21] S. B. Pope, *Turbulent Flows*, IOP Publishing, Bristol, UK, 2001, https://doi.org/10.1017/CBO9780511840531.

[22] R. C. Prince and J. D. Butler, *A protocol for assessing the effectiveness of oil spill dispersants in stimulating the biodegradation of oil*, Environ. Sci. Pollut. Res., 21 (2014), pp. 9506–9510, https://doi.org/10.1007/s11356-013-2053-7.

[23] C. Tsouris and L. L. Tavlarides, *Breakage and coalescence models for drops in turbulent dispersions*, Amer. Inst. Chem. Eng. J., 40 (1994), pp. 395–406, https://doi.org/10.1002/aic.690400303.

[24] L. Zhao, M. C. Boufadel, E. Adams, S. A. Socolofsky, T. King, K. Lee, and T. Nedwed, *Simulation of scenarios of oil droplet formation from the deepwater horizon blowout*, Marine Pollut. Bull., 101 (2015), pp. 304–319, https://doi.org/10.1016/j.marpolbul.2015.10.068.

[25] L. Zhao, M. C. Boufadel, S. A. Socolofsky, E. Adams, T. King, and K. Lee, *Evolution of droplets in subsea oil and gas blowouts: Development and validation of the numerical model VDROP-J*, Marine Pollut. Bull., 83 (2014), pp. 58–69, https://doi.org/10.1016/j.marpolbul.2014.04.020.

[26] L. Zhao, J. Torlapati, M. C. Boufadel, T. King, B. Robinson, and K. Lee, *VDROP: A comprehensive model for droplet formation of oils and gases in liquids-incorporation of the interfacial tension and droplet viscosity*, Chem. Eng. J., 253 (2014), pp. 93–106, https://doi.org/10.1016/j.cej.2014.04.082.